Modeling of Spherical Magnet Arrays Using the Magnetic Charge Model

B. vanNinhuijs, T. E. Motoasca, B. L. J. Gysen, and E. A. Lomonova

Eindhoven University of Technology, Eindhoven MB 5600, The Netherlands

This paper presents an analytical method for evaluating the magnetic flux density produced by spherical permanent magnet arrays used in spherical actuators. To investigate the performances of magnetic arrays, analytical models are used due to their lower computational time compared to 3-D finite element analysis. This paper presents an analytical model for the calculation of the magnetic field produced by a spherical permanent magnet array using magnetic charge modeling. To obtain the total magnetic field solution, first the magnetic field produced by a single spherical tile is considered. By means of superposition, the magnetic field produced by the array is obtained. Two magnet array topologies are modeled and the analytical results are validated using finite element analysis.

***Index Terms*—Analytical modeling, magnetic charge modeling, spherical permanent magnet array.**

I. Introduction

MULTIPLE-DEGREE of freedom actuators are investigated more and more due their smaller size and often more efficient operation than a combination of one-degree of freedom actuators. An example of a multiple-degree of freedom machine is a spherical actuator, which is capable of mimicking a ball and socket joint for such use as robotic applications.

Depending on the desired performance, various spherical actuator topologies can be realized. A spherical actuator consists of a spherical permanent magnet array, as shown in Fig. 1, and a set of coils surrounding this array [1]–[5]. To evaluate its performance, a 3-D finite element analysis (FEA) software is often necessary due to the asymmetrical structure of the actuator. This method is accurate but also very time consuming, especially for a design and optimization of novel topologies. Therefore, analytical models (AMs) that can provide a fast and accurate calculation of the magnetic spatial field distribution [6] are a better alternative.

To obtain the spatial distribution of the magnetic field produced by a spherical permanent magnet array, several analytical models are developed, of which the most well-known ones are the magnetic equivalent circuit model (MEC) [8], the harmonic model [3], and the distributed multipole (DMP) model [9]. Another alternative is to use the magnetic charge model [7], which is presented in this paper. In the MEC models, a lumped element network for the magnetic circuit is created for every permanent magnet (PM) topology. The changes in PM topology, e.g., number and magnetization direction of individual PMs, require construction of a new MEC model. Hence, this technique is not so suitable for design and optimization. The harmonic model can only take a limited number of harmonics into account [10], while the magnetic charge accounts for all the harmonics in the magnetization vectors and in the produced magnetic fields. The DMP model defines the magnetic charge of every dipole where charge modeling is a more general implementation which only considers the volume and surface geometries.

This paper presents the magnetic charge modeling technique in Section II. In Section III, the charge model of a spherical tile is derived, where the complete solution of the spherical permanent magnet array is obtained using superposition. The results obtained from the analytical model are then validated using 3-D FEA software for two examples in Section IV. Finally, conclusions are shown in Section V.

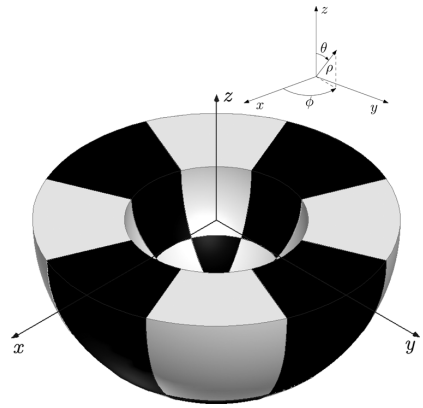

Fig. 1. Section (cutoff) view of a spherical permanent magnet array.

II. Magnetic Charge Model

The magnetic charge model is used to obtain the spatial distribution of the magnetic flux density produced by spherical shaped permanent magnet arrays. With this technique the permanent magnets are replaced by an equivalent spatial (volume or surface) distribution of "magnetic charges" [11]. To find the complete solution for the distributed magnetic flux density, first a single spherical tile is calculated as shown in Fig. 2(a). By means of superposition, the complete solution of the magnetic flux density from the spherical permanent magnet array is obtained. For the presented model, it is assumed that the permanent magnets are uniformly magnetized and have a relative permeability of $\mu_r = 1$. Note that with this assumption, a small error is made because permanent magnets usually have a relative permeability in the order of 1.03–1.05 [12].

Using the Maxwell equations together with the constitutive relation

$$\vec{B} = \mu_0 \vec{H} + \vec{M} \tag{1}$$

expressing the magnetic field strength $\vec{H}$ in terms of a magnetic scalar potential

$$\vec{H} = -\nabla \varphi_m \tag{2}$$

Manuscript received October 30, 2012; accepted December 11, 2012. Date of publication December 19, 2012; date of current version July 15, 2013. Corresponding author: B. van Ninhuijs (e-mail: b.v.ninhuijs@tue.nl).

Color versions of one or more of the figures in this paper are available online at http://ieeexplore.ieee.org.

Digital Object Identifier 10.1109/TMAG.2012.2235411

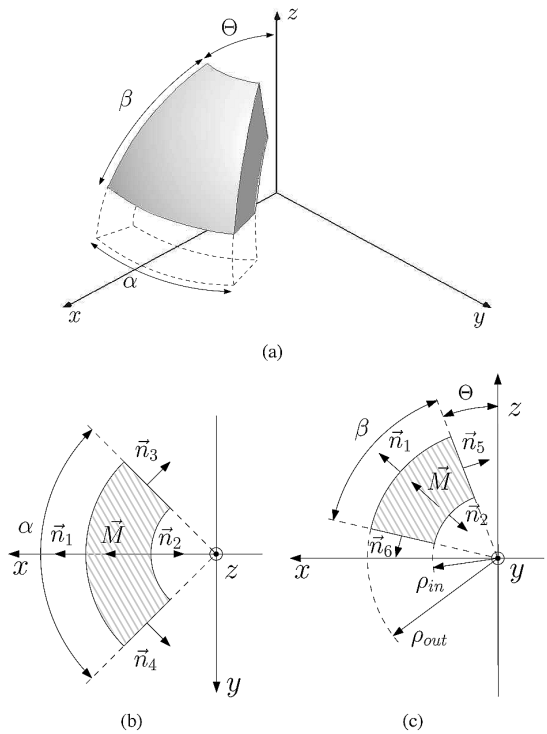

Fig. 2. (a) Spherical tile, (b) top view of the spherical tile, and (c) side view of the spherical tile.

it can be found that

$$\nabla^2 \varphi_m = \nabla \cdot \vec{M} \tag{3}$$

where φ_m is the magnetic scalar potential and $\vec{M}$ is the magnetization vector. Solving this Poisson equation using the free space Green's function will result in

$$\varphi_m(\vec{r}) = \frac{1}{4\pi} \int\limits_V \frac{\rho_m}{|\vec{r} - \vec{r'}|} dv(\vec{r'}) + \frac{1}{4\pi} \oint\limits_S \frac{\sigma_m}{|\vec{r} - \vec{r'}|} ds(\vec{r'}) \tag{4}$$

where $\vec{r} = \rho\vec{e}_\rho + \theta\vec{e}_\theta + \phi\vec{e}_\phi$ is the position vector of an observation point in free space, $\vec{r'}$ is the position vector to each magnetic source point on the magnetic geometry surfaces, and

$$\rho_m = -\nabla' \cdot \vec{M}(\vec{r'}) = 0 \tag{5}$$

is the magnetic volume charge density which is zero because the magnets are considered to be uniformly magnetized, and

$$\sigma_m = \vec{M} \cdot \vec{n} \tag{6}$$

is the magnetic surface charge density, $\vec{n}$ is the normal vector on a closed surface of the spherical magnet tile, as shown in Fig. 2(b) and (c).

III. Magnetic Field Calculation

The magnetic flux density at the observation point outside the magnet can be obtained using

$$\vec{B}(\vec{r}) = \mu_0 \vec{H}, \tag{7}$$

$$= \mu_0(-\nabla\varphi_m), \tag{8}$$

$$= -\frac{\mu_0}{4\pi} \nabla \oint\limits_S \frac{\vec{M}(\vec{r'}) \cdot \vec{n}}{|\vec{r} - \vec{r'}|} ds(\vec{r'}), \tag{9}$$

$$= -\frac{\mu_0}{4\pi} \oint\limits_S \vec{M}(\vec{r'}) \cdot \vec{n}\, \nabla \frac{1}{|\vec{r} - \vec{r'}|} ds(\vec{r'}). \tag{10}$$

Due to the spherical geometry, the solution is defined in the spherical coordinate system using

$$\nabla \frac{1}{|\vec{r} - \vec{r'}|} = -\frac{1}{2} \frac{1}{a^{\frac{3}{2}}} \left[\frac{\partial a}{\partial \rho} \vec{e}_\rho + \frac{1}{\rho} \frac{\partial a}{\partial \theta} \vec{e}_\theta + \frac{1}{\rho \sin(\theta)} \frac{\partial a}{\partial \phi} \vec{e}_\phi \right] \tag{11}$$

where

$$a = \rho^2 + \rho'^2 - 2\rho\rho' \left[\sin(\theta)\sin(\theta')\cos(\phi - \phi') + \cos(\theta)\cos(\theta') \right]. \tag{12}$$

The outer closed surface of the spherical tile can be divided in six surfaces, each with its own normal vector $\vec{n}$ as shown in Fig. 2(b) and (c). These normal vectors are defined in the Cartesian coordinate system as

$$\vec{n}_1 = \begin{bmatrix} \sin(\theta)\cos(\phi)\vec{e}_x \\ \sin(\theta)\sin(\phi)\vec{e}_y \\ \cos(\theta)\vec{e}_z \end{bmatrix} \tag{13}$$

$$\vec{n}_2 = \begin{bmatrix} -\sin(\theta)\cos(\phi)\vec{e}_x \\ -\sin(\theta)\sin(\phi)\vec{e}_y \\ -\cos(\theta)\vec{e}_z \end{bmatrix} \tag{14}$$

$$\vec{n}_3 = \begin{bmatrix} -\sin\left(\frac{\alpha}{2}\right)\vec{e}_x \\ -\cos\left(\frac{\alpha}{2}\right)\vec{e}_y \\ 0 \end{bmatrix} \tag{15}$$

$$\vec{n}_4 = \begin{bmatrix} -\sin\left(\frac{\alpha}{2}\right)\vec{e}_x \\ \cos\left(\frac{\alpha}{2}\right)\vec{e}_y \\ 0 \end{bmatrix} \tag{16}$$

$$\vec{n}_5 = \begin{bmatrix} -\cos(\Theta)\cos(\phi)\vec{e}_x \\ -\cos(\Theta)\sin(\phi)\vec{e}_y \\ \sin(\Theta)\vec{e}_z \end{bmatrix} \tag{17}$$

$$\vec{n}_6 = \begin{bmatrix} \cos(\Theta+\beta)\cos(\phi)\vec{e}_x \\ \cos(\Theta+\beta)\sin(\phi)\vec{e}_y \\ -\sin(\Theta+\beta)\vec{e}_z \end{bmatrix} \tag{18}$$

where α is the angular width of the tile defined in the xy-plane, Θ is the offset angle in the θ-direction, and β is the angular height of the tile in the θ-direction. Since only a uniform magnetization is considered only parallel magnetization can be modeled. The parallel magnetization vector $\vec{M}$ is directed through the middle of the spherical tile as indicated in Fig. 2(b) and (c), while the magnetization vector at any point inside the permanent magnet is defined as

$$\vec{M} = \begin{bmatrix} M_x\vec{e}_x \\ M_y\vec{e}_y \\ M_z\vec{e}_z \end{bmatrix} \tag{19}$$

with

$$M_x = M_0 \sin(\gamma)\cos(\lambda) \tag{20}$$

$$M_y = M_0 \sin(\gamma)\sin(\lambda) \tag{21}$$

$$M_z = M_0 \cos(\gamma) \tag{22}$$

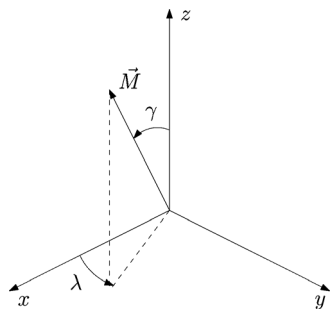

Fig. 3. Direction parameters of the magnetization vector $\vec{M}$.

where γ is the position angle in the θ-direction and λ is the position angle in the ϕ-direction as shown in Fig. 3, and

$$M_0 = \frac{B_{rem}}{\mu_0}. \tag{23}$$

The (23) together with (6) results in for the magnetic surface charge densities

$$\begin{aligned}
\sigma_{m1} &= M_x \sin(\theta)\cos(\phi) + M_y \sin(\theta)\sin(\phi) \\
&\quad + M_z \cos(\theta) && (24)\\
\sigma_{m2} &= -\sigma_{m1} && (25)\\
\sigma_{m3} &= -M_x \sin\left(\frac{\alpha}{2}\right) - M_y \cos\left(\frac{\alpha}{2}\right) && (26)\\
\sigma_{m4} &= -M_x \sin\left(\frac{\alpha}{2}\right) + M_y \cos\left(\frac{\alpha}{2}\right) && (27)\\
\sigma_{m5} &= -M_x \cos(\Theta)\cos(\phi) - M_y \cos(\Theta)\sin(\phi) \\
&\quad + M_z \sin(\Theta) && (28)\\
\sigma_{m6} &= -\sigma_{m5}. && (29)
\end{aligned}$$

Using (10) and

$$ds(\vec{r'}) = \begin{cases} \rho'^2 \sin(\theta')d\theta' d\phi' & \text{if } \rho' \text{ is constant} \\ \rho' \sin(\theta')d\rho' d\phi' & \text{if } \theta' \text{ is constant} \\ \rho' d\rho' d\theta' & \text{if } \phi' \text{ is constant} \end{cases} \tag{30}$$

the resulting magnetic flux density on the surfaces of the tile can be obtained as

$$\begin{aligned}
\vec{B}_{1,2} &= -\frac{\mu_0}{4\pi} \int_{-\frac{\alpha}{2}}^{\frac{\alpha}{2}} \int_{\Theta}^{\Theta+\beta} \sigma_{m1,2} \nabla \frac{1}{|\vec{r} - \vec{r'}|} \\
&\quad \times \rho'^2 \sin(\theta') d\theta' d\phi', && (31)\\
\vec{B}_{3,4} &= -\frac{\mu_0}{4\pi} \int_{-\frac{\alpha}{2}}^{\frac{\alpha}{2}} \int_{\rho_{in}}^{\rho_{out}} \sigma_{m3,4} \nabla \frac{1}{|\vec{r} - \vec{r'}|} \\
&\quad \times \rho' \sin(\Theta) d\rho' d\phi', && (32)\\
\vec{B}_{5,6} &= -\frac{\mu_0}{4\pi} \int_{\Theta}^{\Theta+\beta} \int_{\rho_{in}}^{\rho_{out}} \sigma_{m5,6} \nabla \frac{1}{|\vec{r} - \vec{r'}|} \\
&\quad \times \rho' d\rho' d\theta'. && (33)
\end{aligned}$$

The total magnetic flux density, generated by the spherical tile, is the summation of the individual magnetic flux densities hence

$$\vec{B}(\rho, \theta, \phi) = \vec{B}_1 + \vec{B}_2 + \vec{B}_3 + \vec{B}_4 + \vec{B}_5 + \vec{B}_6. \tag{34}$$

In a similar way, the magnetic flux density of the other spherical tiles of the spherical permanent magnet array can be determined. By means of superposition, the magnetic field produced by the complete array is obtained.

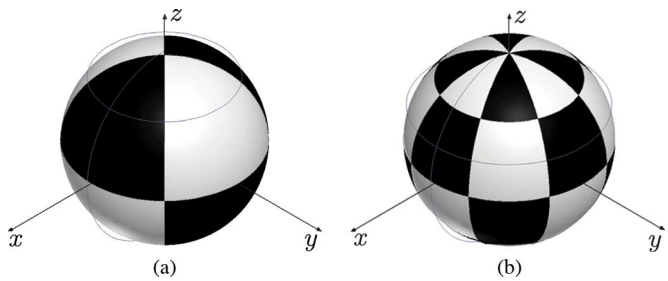

Fig. 4. Developed FEA model with (a) 8 magnets and (b) 32 magnets.

TABLE I
GEOMETRIC PARAMETERS OF THE SPHERICAL PERMANENT MAGNET ARRAY

Parameter	Value	Unit	Description
ρ_{out}	10	mm	Outer radius of the tile
ρ_{in}	5	mm	Inner radius of the tile
B_{rem}	1.23	T	Remanent flux density of the magnet
μ_r	1	-	Relative permeability of the magnet
α	90 & 45	deg	Angle width considering 8 & 32 PMs
β	90 & 45	deg	Angle height considering 8 & 32 PMs
Θ	0 & 0	deg	Offset angle considering 8 & 32 PMs

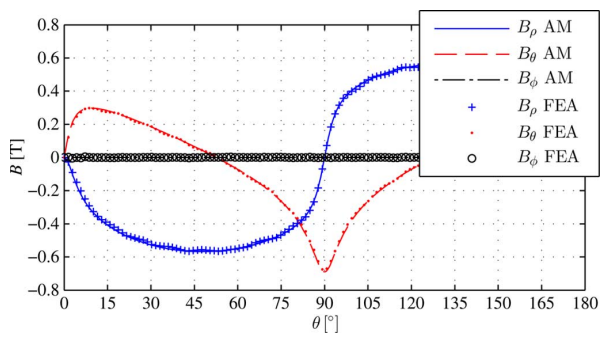

Fig. 5. Spatial distribution of the magnetic flux density at $\rho = 10.5$ mm and $\phi = 0°$ of the analytical model (AM) and FEA, considering 8 magnets.

IV. FINITE ELEMENT VERIFICATION

To validate the analytical results, a FEA software package from Ansys, Maxwell 15 is used. Two spherical permanent magnet array topologies are validated, one with 8 permanent magnets in total, and one with 32 permanent magnets in total, as shown in Fig. 4(a) and (b), respectively. The geometric parameters chosen for this validation are stated in Table I. The relative error of the magnetic flux density is defined as

$$E_r = \frac{rms(B_{AM} - B_{FEA})}{rms(B_{FEA})} \tag{35}$$

where B_{AM} is the magnetic flux density of the analytical model, and B_{FEA} is the magnetic flux density of the FEA results.

The spatial distribution of the magnetic flux density for the permanent magnet array with 8 permanent magnets at $\phi = 0°$ and $\rho = 10.5$ mm in the θ-direction is shown in Fig. 5. Additionally, the spatial distribution of the magnetic flux density in the ϕ-direction at $\theta = 45°$ and $\rho = 10.5$ mm is shown

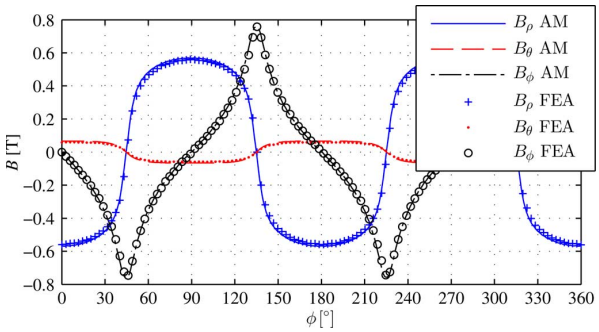

Fig. 6. Spatial distribution of the magnetic flux density at $\rho = 10.5$ mm and $\theta = 45°$ of the analytical model (AM) and FEA, considering 8 magnets.

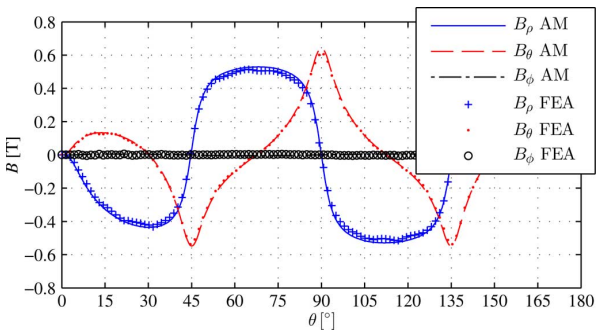

Fig. 7. Spatial distribution of the magnetic flux density at $\rho = 10.5$ mm and $\phi = 0°$ of the analytical model (AM) and FEA, considering 32 magnets.

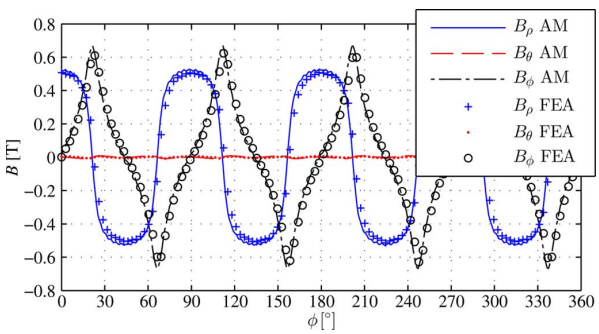

Fig. 8. Spatial distribution of the magnetic flux density at $\rho = 10.5$ mm and $\theta = 67.5°$ of the analytical model (AM) and FEA, considering 32 magnets.

in Fig. 6. In both figures, it can be observed that the analytical model and FEA results are in very good agreement with the error being less than 3%.

For the spherical permanent magnet array containing 32 magnets, the spatial magnetic flux density distribution at $\phi = 0°$ and $\rho = 10.5$ mm in the θ-direction is shown in Fig. 7. The spatial magnetic flux density distribution in the ϕ-direction at $\theta = 67.5°$ and $\rho = 10.5$ mm is shown in Fig. 8. In both figures, discretization in the FEA results can be observed. In spite of this discretization, the analytical and FEA results are in good agreement, with a relative error of less than 3%. It can be concluded that the analytical model is accurate for different sized spherical permanent magnet arrays.

V. Conclusion

This paper has presented an analytical model based on the magnetic charge density representation of permanent magnets to obtain the complete spatial magnetic flux density of a spherical tile. By means of superposition, the complete 3-D solution of a spherical permanent magnet array has been obtained. Two spherical permanent magnet arrays have been implemented, one with 8 permanent magnets and one with 32 permanent magnets. The results from the analytical model have been compared with 3-D FEA, and an agreement with a relative error less than 3% has been found. Therefore, this method gives a fast and accurate alternative to 3-D FEA for finding the magnetic flux density produced by spherical permanent magnet arrays and can be used for accurate force and torque predictions. Further, due to the flexibility of the model, the magnetic flux density generated by the spherical permanent magnet array can be predicted for different geometry parameters, permanent magnet array sizes, and tile arrangements.

Acknowledgment

This work has received funding from the Dutch "Pieken in de Delta" Program, Project McArm PID102055.

References

[1] H. Li, C. Xia, and T. Shi, "Spherical harmonic analysis of a novel Halbach array PM spherical motor," in *Proc. IEEE Int. Conf. Robot. Biomimetics. ROBIO.*, 2007, pp. 2085–2089.

[2] H. Son and K.-M. Lee, "Open-loop controller design and dynamic characteristics of a spherical wheel motor," *IEEE Trans. Ind. Electron.*, vol. 57, no. 10, pp. 3475–3482, Oct. 2010.

[3] W. Wang, J. Wang, G. Jewell, and D. Howe, "Design and control of a novel spherical permanent magnet actuator with three degrees of freedom," *Trans. on Mechatron., IEEE/ASME*, vol. 8, no. 4, pp. 457–468, 2003.

[4] T. Yano, Y. Kubota, T. Shikayama, and T. Suzuki, "Basic characteristics of a multi-pole spherical synchronous motor," in *Proc. Int. Symp. Micro-NanoMechatron. Human Sci.*, 2007, pp. 383–388.

[5] L. Yan, I.-M. Chen, C. K. Lim, G. Yang, W. Lin, and K.-M. Lee, "Design and analysis of a permanent magnet spherical actuator," in *Proc. IEEE/RSJ Int. Conf. Intell. Robots Syst. (IROS)*, 2005, pp. 691–696.

[6] J. Janssen, J. Paulides, and E. Lomonova, "Three-dimensional analytical field calculation of pyramidal-frustum shaped permanent magnets," *IEEE Trans. Magn.*, vol. 45, no. 10, pp. 4628–4631, Oct. 2009.

[7] J. C. Compter, E. A. Lomonova, and J. Makarovic, "Direct 3-D method for performance prediction of a linear moving coil actuator with various topologies," in *Proc. IEE Sci., Measur., Technol.* , Jul. 2003, vol. 150, no. 4, pp. 183–191.

[8] B. Li, G.-D. Li, and H.-F. Li, "Magnetic field analysis of 3-DOF permanent magnetic spherical motor using magnetic equivalent circuit method," *IEEE Trans. Magn.*, vol. 47, no. 8, pp. 2127–2133, Aug. 2011.

[9] K.-M. Lee and H. Son, "Distributed multipole model for design of permanent-magnet-based actuators," *IEEE Trans. Magn.*, vol. 43, no. 10, pp. 3904–3913, Oct. 2007.

[10] B. van Ninhuijs, T. Motoasca, and E. Lomonova, "Accurate analytical computation of magnetic flux density of spherical permanent magnet arrays," in *Proc. IEEE Int. Conf. Electr. Mach. (ICEM)*, Sep. 2012, pp. 2746–2751.

[11] E. P. Furlani, *Permanent Magnet and Electromechanical Devices*. Rochester, NY, USA: Academic Press, 2001.

[12] J. Janssen, J. Paulides, and E. Lomonova, "3D analytical calculation of the torque between perpendicular magnetized magnets in magnetic suspensions," *IEEE Trans. Magn.*, vol. 47, no. 10, pp. 4286–4289, Oct. 2011.